CLEO CONF 00-6
ICHEP 00-552

Study of χ_{c1} and χ_{c2} meson production in B meson decays

CLEO Collaboration

(July 27, 2000)

Abstract

Using a sample of 9.7×10^6 $B\overline{B}$ meson pairs collected with the CLEO detector, we study inclusive B meson decays to the χ_{c1} and χ_{c2} charmonia states. We measure the branching fraction for the inclusive χ_{c1} production in B decays to be $\mathcal{B}(B \to \chi_{c1} X) = (4.14 \pm 0.31 \pm 0.40) \times 10^{-3}$, where the first uncertainty is statistical and the second one is systematic. We obtain the branching fractions for direct χ_{c1} and χ_{c2} production in B decays by subtracting the contribution from the decay chain $B \to \psi(2S)X$ with $\psi(2S) \to \chi_{c1,2}\gamma$. We measure $\mathcal{B}(B \to \chi_{c1}[\text{direct}]X) = (3.83\pm 0.31\pm 0.40)\times 10^{-3}$. No statistically significant signal for χ_{c2} production is observed in either case. We determine the 95% C.L. upper limits to be $\mathcal{B}(B \to \chi_{c2} X) < 2.0 \times 10^{-3}$, $\mathcal{B}(B \to \chi_{c2}[\text{direct}]X) < 1.7 \times 10^{-3}$, and $\mathcal{B}(B \to \chi_{c2}[\text{direct}]X)/\mathcal{B}(B \to \chi_{c1}[\text{direct}]X) < 0.44$. All quoted results are preliminary.

Submitted to XXXth International Conference on High Energy Physics, July 2000, Osaka, Japan

G. Brandenburg,[1] A. Ershov,[1] Y. S. Gao,[1] D. Y.-J. Kim,[1] R. Wilson,[1] T. E. Browder,[2] Y. Li,[2] J. L. Rodriguez,[2] H. Yamamoto,[2] T. Bergfeld,[3] B. I. Eisenstein,[3] J. Ernst,[3] G. E. Gladding,[3] G. D. Gollin,[3] R. M. Hans,[3] E. Johnson,[3] I. Karliner,[3] M. A. Marsh,[3] M. Palmer,[3] C. Plager,[3] C. Sedlack,[3] M. Selen,[3] J. J. Thaler,[3] J. Williams,[3] K. W. Edwards,[4] R. Janicek,[5] P. M. Patel,[5] A. J. Sadoff,[6] R. Ammar,[7] A. Bean,[7] D. Besson,[7] R. Davis,[7] N. Kwak,[7] X. Zhao,[7] S. Anderson,[8] V. V. Frolov,[8] Y. Kubota,[8] S. J. Lee,[8] R. Mahapatra,[8] J. J. O'Neill,[8] R. Poling,[8] T. Riehle,[8] A. Smith,[8] C. J. Stepaniak,[8] J. Urheim,[8] S. Ahmed,[9] M. S. Alam,[9] S. B. Athar,[9] L. Jian,[9] L. Ling,[9] M. Saleem,[9] S. Timm,[9] F. Wappler,[9] A. Anastassov,[10] J. E. Duboscq,[10] E. Eckhart,[10] K. K. Gan,[10] C. Gwon,[10] T. Hart,[10] K. Honscheid,[10] D. Hufnagel,[10] H. Kagan,[10] R. Kass,[10] T. K. Pedlar,[10] H. Schwarthoff,[10] J. B. Thayer,[10] E. von Toerne,[10] M. M. Zoeller,[10] S. J. Richichi,[11] H. Severini,[11] P. Skubic,[11] A. Undrus,[11] S. Chen,[12] J. Fast,[12] J. W. Hinson,[12] J. Lee,[12] D. H. Miller,[12] E. I. Shibata,[12] I. P. J. Shipsey,[12] V. Pavlunin,[12] D. Cronin-Hennessy,[13] A.L. Lyon,[13] E. H. Thorndike,[13] C. P. Jessop,[14] M. L. Perl,[14] V. Savinov,[14] X. Zhou,[14] T. E. Coan,[15] V. Fadeyev,[15] Y. Maravin,[15] I. Narsky,[15] R. Stroynowski,[15] J. Ye,[15] T. Wlodek,[15] M. Artuso,[16] R. Ayad,[16] C. Boulahouache,[16] K. Bukin,[16] E. Dambasuren,[16] S. Karamov,[16] G. Majumder,[16] G. C. Moneti,[16] R. Mountain,[16] S. Schuh,[16] T. Skwarnicki,[16] S. Stone,[16] G. Viehhauser,[16] J.C. Wang,[16] A. Wolf,[16] J. Wu,[16] S. Kopp,[17] A. H. Mahmood,[18] S. E. Csorna,[19] I. Danko,[19] K. W. McLean,[19] Sz. Márka,[19] Z. Xu,[19] R. Godang,[20] K. Kinoshita,[20,*] I. C. Lai,[20] S. Schrenk,[20] G. Bonvicini,[21] D. Cinabro,[21] S. McGee,[21] L. P. Perera,[21] G. J. Zhou,[21] E. Lipeles,[22] S. P. Pappas,[22] M. Schmidtler,[22] A. Shapiro,[22] W. M. Sun,[22] A. J. Weinstein,[22] F. Würthwein,[22,†] D. E. Jaffe,[23] G. Masek,[23] H. P. Paar,[23] E. M. Potter,[23] S. Prell,[23] D. M. Asner,[24] A. Eppich,[24] T. S. Hill,[24] R. J. Morrison,[24] R. A. Briere,[25] G. P. Chen,[25] B. H. Behrens,[26] W. T. Ford,[26] A. Gritsan,[26] J. Roy,[26] J. G. Smith,[26] J. P. Alexander,[27] R. Baker,[27] C. Bebek,[27] B. E. Berger,[27] K. Berkelman,[27] F. Blanc,[27] V. Boisvert,[27] D. G. Cassel,[27] M. Dickson,[27] P. S. Drell,[27] K. M. Ecklund,[27] R. Ehrlich,[27] A. D. Foland,[27] P. Gaidarev,[27] L. Gibbons,[27] B. Gittelman,[27] S. W. Gray,[27] D. L. Hartill,[27] B. K. Heltsley,[27] P. I. Hopman,[27] C. D. Jones,[27] D. L. Kreinick,[27] M. Lohner,[27] A. Magerkurth,[27] T. O. Meyer,[27] N. B. Mistry,[27] E. Nordberg,[27] J. R. Patterson,[27] D. Peterson,[27] D. Riley,[27] J. G. Thayer,[27] D. Urner,[27] B. Valant-Spaight,[27] A. Warburton,[27] P. Avery,[28] C. Prescott,[28] A. I. Rubiera,[28] J. Yelton,[28] and J. Zheng[28]

[1]Harvard University, Cambridge, Massachusetts 02138
[2]University of Hawaii at Manoa, Honolulu, Hawaii 96822
[3]University of Illinois, Urbana-Champaign, Illinois 61801
[4]Carleton University, Ottawa, Ontario, Canada K1S 5B6
and the Institute of Particle Physics, Canada
[5]McGill University, Montréal, Québec, Canada H3A 2T8
and the Institute of Particle Physics, Canada

[*]Permanent address: University of Cincinnati, Cincinnati, OH 45221

[†]Permanent address: Massachusetts Institute of Technology, Cambridge, MA 02139.

[6]Ithaca College, Ithaca, New York 14850
[7]University of Kansas, Lawrence, Kansas 66045
[8]University of Minnesota, Minneapolis, Minnesota 55455
[9]State University of New York at Albany, Albany, New York 12222
[10]Ohio State University, Columbus, Ohio 43210
[11]University of Oklahoma, Norman, Oklahoma 73019
[12]Purdue University, West Lafayette, Indiana 47907
[13]University of Rochester, Rochester, New York 14627
[14]Stanford Linear Accelerator Center, Stanford University, Stanford, California 94309
[15]Southern Methodist University, Dallas, Texas 75275
[16]Syracuse University, Syracuse, New York 13244
[17]University of Texas, Austin, TX 78712
[18]University of Texas - Pan American, Edinburg, TX 78539
[19]Vanderbilt University, Nashville, Tennessee 37235
[20]Virginia Polytechnic Institute and State University, Blacksburg, Virginia 24061
[21]Wayne State University, Detroit, Michigan 48202
[22]California Institute of Technology, Pasadena, California 91125
[23]University of California, San Diego, La Jolla, California 92093
[24]University of California, Santa Barbara, California 93106
[25]Carnegie Mellon University, Pittsburgh, Pennsylvania 15213
[26]University of Colorado, Boulder, Colorado 80309-0390
[27]Cornell University, Ithaca, New York 14853
[28]University of Florida, Gainesville, Florida 32611

The recent measurements of charmonium production in various high-energy physics reactions have brought welcome surprises and challenged our understanding both of heavy-quark production and of quarkonium bound state formation. The measurement of a large production rate of high-P_T charmonium at the Tevatron [1] was in sharp disagreement with the then-standard color-singlet model. The development of the NRQCD factorization framework [2] has put the calculations of the inclusive charmonium production on a rigorous footing. The high-P_T charmonium production rate at the Tevatron is now well understood in this formalism. The recent CDF measurement of charmonium polarization [3], however, appears to disagree with the NRQCD prediction. The older color-evaporation model accommodates both the high-P_T charmonium production rate and polarization measurements at the Tevatron [4].

Inclusive B meson decays to charmonia is another area to confront theoretical predictions with experimental data. The color-singlet contribution, for example, is a factor of 5–10 below [5] the observed inclusive J/ψ production rate [6]. A measurement of the χ_{c2}-to-χ_{c1} production ratio in B decays provides an especially clean test of the charmonium production models. The $V-A$ current $\overline{c}\gamma_\mu(1-\gamma_5)c$ cannot create a $c\overline{c}$ pair in a ${}^{2S+1}L_J = {}^3P_2$ state, therefore the decay $B \to \chi_{c2}X$ is forbidden at leading order in α_s in the color-singlet model [7]. The importance of the color-octet mechanism for the χ_c production in B decays was recognized [8] even before the development of the NRQCD framework. The NRQCD calculations of the B decays to charmonia at the next-to-leading order in α_s can be found in Ref. [5]. The color-octet contribution to $B \to \chi_{cJ}X$ decays is proportional to $2J+1$. Therefore, if this mechanism dominates, then the χ_{c2}-to-χ_{c1} production ratio should be 5:3. On the contrary, if the color-singlet contribution dominates, then the ratio should be 0:1. The color-evaporation model predicts $\chi_{c2} : \chi_{c1} = 5 : 3$ [9].

Our data were collected at the Cornell Electron Storage Ring (CESR) with two configurations of the CLEO detector called CLEO II [10] and CLEO II.V [11]. The components of the CLEO detector most relevant to this analysis are the charged particle tracking system, the CsI electromagnetic calorimeter, and the muon chambers. In CLEO II the momenta of charged particles are measured in a tracking system consisting of a 6-layer straw tube chamber, a 10-layer precision drift chamber, and a 51-layer main drift chamber, all operating inside a 1.5 T solenoidal magnet. The main drift chamber also provides a measurement of the specific ionization, dE/dx, used for particle identification. For CLEO II.V, the straw tube chamber was replaced with a 3-layer silicon vertex detector, and the gas in the main drift chamber was changed from an argon-ethane to a helium-propane mixture. The muon chambers consist of proportional counters placed at increasing depth in the steel absorber.

We use 9.2 fb^{-1} of e^+e^- data taken at the $\Upsilon(4S)$ resonance and 4.6 fb^{-1} taken 60 MeV below the $\Upsilon(4S)$ resonance (off-$\Upsilon(4S)$ sample). Two thirds of the data were collected with the CLEO II.V detector. The simulated event samples used in this analysis were generated with a GEANT-based [12] simulation of the CLEO detector response and were processed in a similar manner as the data.

We reconstruct the χ_{c1} and χ_{c2} radiative decays to J/ψ. The branching fractions for the $\chi_{c1,2} \to J/\psi\,\gamma$ decays are, respectively, $(27.3 \pm 1.6)\%$ and $(13.5 \pm 1.1)\%$ [13], whereas the branching fraction for the $\chi_{c0} \to J/\psi\,\gamma$ decay is only $(0.66 \pm 0.18)\%$. In addition, the χ_{c0} production rate in B decays is expected to be smaller than the $\chi_{c1,2}$ rates [5,8]. We therefore do not attempt to measure χ_{c0} production in this analysis.

We reconstruct both $J/\psi \to e^+e^-$ and $J/\psi \to \mu^+\mu^-$ decays. Electron candidates are identified based on the ratio of the track momentum to the associated shower energy in the CsI calorimeter and on the dE/dx measurement. The internal bremsstrahlung in the $J/\psi \to e^+e^-$ decay as well as the bremsstrahlung in the detector material produces a long radiative tail in the e^+e^- invariant mass distribution and impedes efficient $J/\psi \to e^+e^-$ detection. We recover some of the bremsstrahlung photons by selecting the photon shower with the smallest opening angle with respect to the direction of the $e^\pm$ track evaluated at the interaction point, and then requiring this opening angle to be smaller than 5°. We therefore refer to the $e^+(\gamma)e^-(\gamma)$ invariant mass when we describe the $J/\psi \to e^+e^-$ reconstruction. For the $J/\psi \to \mu^+\mu^-$ reconstruction, one of the muon candidates is required to penetrate the steel absorber to a depth greater than 3 nuclear interaction lengths. We relax the absorber penetration requirement for the second muon candidate if it is not expected to reach a muon chamber either because its energy is too low or because it does not point to a region of the detector covered by the muon chambers. For these muon candidates we require the ionization signature in the CsI calorimeter to be consistent with that of a muon. We use the normalized invariant mass for the J/ψ candidate selection. For example, the normalized $J/\psi \to \mu^+\mu^-$ mass is defined as $[M(\mu^+\mu^-) - M_{J/\psi}]/\sigma(M)$, where $M_{J/\psi}$ is the world average value of the J/ψ mass [13] and $\sigma(M)$ is the calculated mass resolution for that particular $\mu^+\mu^-$ combination. The average $\ell^+\ell^-$ invariant mass resolution is 12 MeV/c^2. The normalized mass distributions for the $J/\psi \to \ell^+\ell^-$ candidates are shown in Fig. 1. We require the normalized mass to be from -6 to $+3$ for the $J/\psi \to e^+e^-$ and from -4 to $+3$ for the $J/\psi \to \mu^+\mu^-$ candidates. The momentum of the J/ψ candidates is required to be less than 2 GeV/c, which is slightly above the maximal J/ψ momentum in B decays.

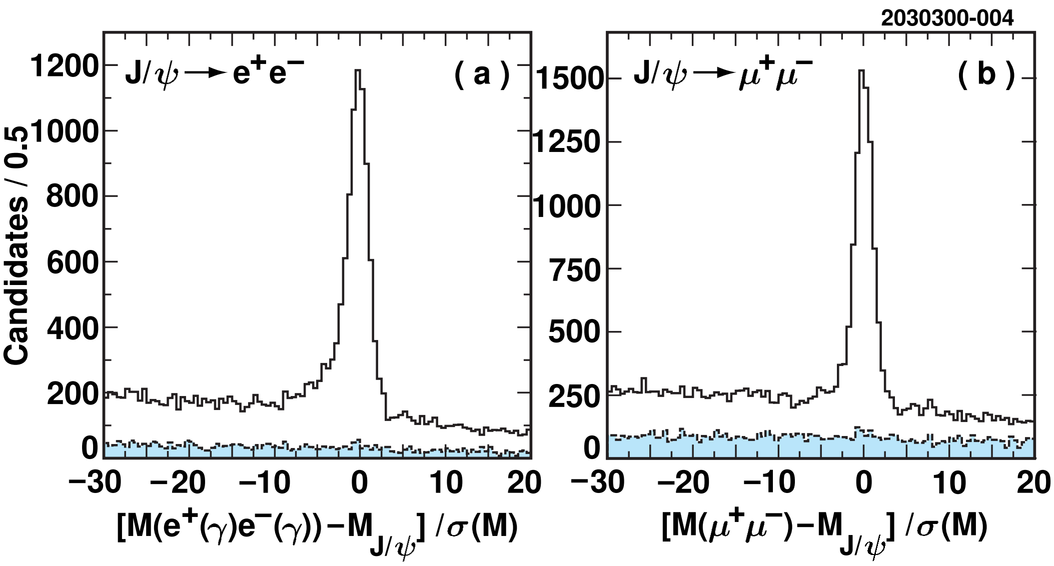

FIG. 1. Normalized invariant mass of the (a) $J/\psi \to e^+e^-$ and (b) $J/\psi \to \mu^+\mu^-$ candidates in the data. The momentum of the J/ψ candidates is required to be less than 2 GeV/c. The shaded histogram represents the luminosity-scaled data taken 60 MeV below the $\Upsilon(4S)$ showing the level of background from non-$B\overline{B}$ events.

Photon candidates for $\chi_{c1,2} \to J/\psi\,\gamma$ reconstruction must be detected in the barrel region of the calorimeter, defined as $|\cos\theta_\gamma| < 0.71$, where θ_γ is the angle between the beam axis and the candidate photon. Most of the photons in $\Upsilon(4S) \to B\overline{B}$ events come from π^0 decays. We therefore do not use a photon for the $\chi_{c1,2} \to J/\psi\,\gamma$ reconstruction if it can be paired with another photon to produce a π^0 candidate with the normalized $\pi^0 \to \gamma\gamma$ mass between -3 and $+2$.

We determine the χ_{c1} and χ_{c2} yields in a maximum-likelihood fit to the mass-difference distribution $M(J/\psi\gamma) - M(J/\psi)$ (Fig. 2), where $M(J/\psi)$ is the measured mass of a J/ψ candidate. The excellent electromagnetic calorimeter allows us to resolve the χ_{c1} and χ_{c2} peaks. The $M(J/\psi\gamma) - M(J/\psi)$ mass-difference resolution is approximately 8 MeV/c^2 and is dominated by the photon energy resolution. The background in the fit is approximated with a 5th order Chebyshev polynomial; all the polynomial coefficients are allowed to float. The χ_{c1} and χ_{c2} signal shapes are fit with templates extracted from Monte Carlo simulation; only the template normalizations are floating in the fit. The χ_{c1} and χ_{c2} signal yields in the $\Upsilon(4S)$ data are $N^{\rm ON}(\chi_{c1}) = 672 \pm 47$[stat] and $N^{\rm ON}(\chi_{c2}) = 83 \pm 37$[stat]. The χ_{c1} and χ_{c2} yields in off-$\Upsilon(4S)$ data are consistent with zero: $N^{\rm OFF}(\chi_{c1}) = 4.1 \pm 7.1$[stat] and $N^{\rm OFF}(\chi_{c2}) = 1.1 \pm 6.5$[stat]. Subtracting the contributions from non-$B\overline{B}$ continuum events, we obtain the total inclusive $B \to \chi_{c1}X$ and $B \to \chi_{c2}X$ yields

$$N(B \to \chi_{c1}X) = 664 \pm 49[\text{stat}] \text{ and } N(B \to \chi_{c2}X) = 81 \pm 39[\text{stat}].$$

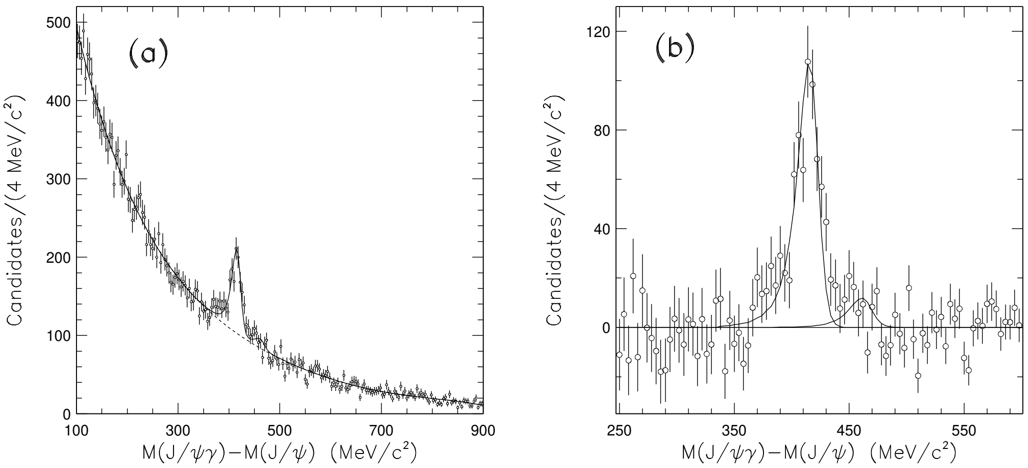

FIG. 2. Plot (a) shows the $M(J/\psi\gamma) - M(J/\psi)$ distribution in the $\Upsilon(4S)$ data (points with error bars). The fit function is shown by a solid line with the background component represented by a dashed line. Plot (b) shows the background-subtracted distribution in the signal region with the χ_{c1} and χ_{c2} fit components represented by a solid line.

Taking into account the systematic uncertainties associated with the fit, we determine the $B \to \chi_{c2}X$ signal yield significance to be 2.0 standard deviations. Subtracting the feeddown from the decay chain $B \to \psi(2S)X$ with $\psi(2S) \to \chi_{c2}\gamma$ and accounting for the associated systematic uncertainty, we likewise determine the significance of the evidence for the direct $B \to \chi_{c2}X$ decays to be 1.4 standard deviations.

To calculate branching fractions for the $B \to \chi_{c1,2}X$ decays, we use the measured signal yields $N(B \to \chi_{c1,2}X)$, reconstruction efficiencies extracted from simulation, the number of produced $B\overline{B}$ pairs, and the daughter branching fractions. For the calculation of the rates for direct $B \to \chi_{c1,2}X$ decays, we make an assumption that the only other source of $\chi_{c1,2}$ meson production in B decays is the decay chain $B \to \psi(2S)X$ with $\psi(2S) \to \chi_{c1,2}\gamma$. The resulting branching fractions are listed in Table I.

TABLE I. The measured branching fractions for inclusive B decays to χ_{c1} and χ_{c2}. We subtract the $\psi(2S) \to \chi_{c1,2}\gamma$ feeddown to arrive at the branching fractions for direct $B \to \chi_{c1,2}X$ decays. The correlation between the uncertainties is taken into account in the calculation of the χ_{c2}-to-χ_{c1} production ratio (last row).

Branching fraction or ratio	Measured value	95% C.L. upper limit [15]
$\mathcal{B}(B \to \chi_{c1}X)$	$(4.14 \pm 0.31 \pm 0.40) \times 10^{-3}$	—
$\mathcal{B}(B \to \chi_{c1}[\text{direct}]X)$	$(3.83 \pm 0.31 \pm 0.40) \times 10^{-3}$	—
$\mathcal{B}(B \to \chi_{c2}X)$	$(0.98 \pm 0.48 \pm 0.15) \times 10^{-3}$	$< 2.0 \times 10^{-3}$ [a]
$\mathcal{B}(B \to \chi_{c2}[\text{direct}]X)$	$(0.71 \pm 0.48 \pm 0.16) \times 10^{-3}$	$< 1.7 \times 10^{-3}$
$\frac{\mathcal{B}(B\to\chi_{c2}[\text{direct}]X)}{\mathcal{B}(B\to\chi_{c1}[\text{direct}]X)}$	$0.18 \pm 0.13 \pm 0.04$	< 0.44

[a] The 95% confidence interval in the "unified" approach [15] is $[0.2; 2.0] \times 10^{-3}$.

The systematic uncertainties are listed in Table II. The sources of the uncertainty can be grouped into three categories:

(i) *Fit procedure.*— This category includes the systematic uncertainties due to the choice of the signal and background shapes as well as the bin size. To fit the χ_{c1} and χ_{c2} signal, we use the templates extracted from simulation. We therefore are sensitive to the imperfections in the simulation of the photon energy measurement. The systematic uncertainties associated with the simulation of the calorimeter response are estimated by comparing the $\pi^0 \to \gamma\gamma$ invariant mass lineshapes for inclusive π^0 candidates in data and Monte Carlo samples. Then we modify the χ_{c1} and χ_{c2} templates to determine the resulting uncertainty in the signal yields. To estimate the uncertainty associated with the calorimeter energy scale, we shift the χ_{c1} and χ_{c2} templates by ± 0.6 MeV/c^2 in the fit. The uncertainty due to time-dependent variations of the calorimeter energy scale is small compared to the overall energy scale uncertainty. To estimate the uncertainty due the calorimeter energy resolution, we change the width of the χ_{c1} and χ_{c2} templates by $\pm 4\%$. The uncertainty in background shape is probed by fitting the background with the template extracted from the high-statistics samples of simulated $\Upsilon(4S) \to B\overline{B}$ and non-$B\overline{B}$ continuum events; only the template normalization, not its shape, is allowed to float in the fit.

(ii) *Efficiency calculation.*— This category includes the uncertainties in the number of produced $B\overline{B}$ pairs, tracking efficiency, photon detection efficiency, lepton detection efficiency, statistical uncertainties of the simulated event samples, and the model-dependence in the simulation of $B \to \chi_{c1,2}X$ decays. The angular distribution of the $\chi_{c1,2} \to J/\psi\gamma$ decays affects the photon energy spectrum. We define the helicity angle θ_h to be the angle between the γ direction in χ_c frame and the χ_c direction in the B frame. We assume flat $\cos\theta_h$ distribution in our simulation of $B \to \chi_{c1,2}X$ decays. Systematic uncertainty associated with this assumption is estimated by comparing the reconstruction efficiencies in the Monte Carlo samples with $I(\theta_h) \propto \sin^2\theta_h$ and $I(\theta_h) \propto \cos^2\theta_h$ angular distributions. Another source of uncertainty is the modeling of the X system in the simulation of $B \to \chi_{c1,2}X$ decays. The photon detection efficiency depends on the assumed model through the χ_c momentum spectrum and the π^0 multiplicity of the final state. In our simulation, we assume that X is either K or one of the higher K resonances: 24% K, 24% $K^*(892)$, 14% $K_1(1270)$, 14% $K_1(1400)$, 13% $K_0^*(1430)$, and 11% $K_2^*(1430)$; we also include the decay chain $B \to \psi(2S)X$ with $\psi(2S) \to \chi_{c1,2}\gamma$. To estimate the systematic uncertainty, we compare the $\chi_c \to J/\psi\gamma$ detection efficiency extracted using this sample with the efficiency in the sample where we assume that X is either a K^+ or $K^0_S \to \pi^+\pi^-$.

(iii) *Assumed branching fractions.*— This category includes the uncertainties on the branching fractions. We use the following values of the daughter branching fractions: $\mathcal{B}(J/\psi \to \ell^+\ell^-) = (5.894 \pm 0.086)\%$ [14], $\mathcal{B}(\chi_{c1} \to J/\psi\gamma) = (27.3 \pm 1.6)\%$ [13], and $\mathcal{B}(\chi_{c2} \to J/\psi\gamma) = (13.5 \pm 1.1)\%$ [13]. In calculation of $\mathcal{B}(B \to \chi_{c1,2}[\text{direct}]X)$ we also assume the following values: $\mathcal{B}(B \to \psi(2S)X) = (3.5 \pm 0.5) \times 10^{-3}$ [13], $\mathcal{B}(\psi(2S) \to \chi_{c1}\gamma) = (8.7 \pm 0.8)\%$ [13], and $\mathcal{B}(\psi(2S) \to \chi_{c2}\gamma) = (7.8 \pm 0.8)\%$ [13].

TABLE II. Systematic uncertainties on the measured branching fractions.

Source of systematic uncertainty	relative uncertainty in % $\mathcal{B}(B \to \chi_{c1}X)$	$\mathcal{B}(B \to \chi_{c2}X)$
(i) Fit procedure		
Calorimeter energy scale	0.4	5.6
Calorimeter energy resolution	2.8	6.9
Background shape	1.8	6.8
Bin size	0.0	1.9
(ii) Efficiency calculation		
$N(B\overline{B})$	2.0	2.0
Tracking efficiency	2.0	2.0
Lepton identification	4.2	4.2
Photon finding	2.5	2.5
Monte Carlo statistics	0.7	0.7
Composition of X in $B \to \chi_{c1,2}X$ simulation	3.3	3.3
Angular distribution for $\chi_{c1,2} \to J/\psi\gamma$	1.0	1.0
(iii) Assumed branching fractions		
$\mathcal{B}(\chi_{c1,2} \to J/\psi\gamma)$	5.9	8.1
$\mathcal{B}(J/\psi \to \ell^+\ell^-)$	1.5	1.5
$\mathcal{B}(B \to \psi(2S)X)$[a]	1.1	5.5
$\mathcal{B}(\psi(2S) \to \chi_{c1,2}\gamma)$[a]	0.7	4.0

[a]Contributes only to uncertainty on $\mathcal{B}(B \to \chi_{c1,2}[\text{direct}]X)$.

In conclusion, we have measured the branching fractions for inclusive B meson decays to χ_{c1} and χ_{c2} charmonia states. Our measurements are consistent with and improve upon the previous CLEO results [6]. Our measurement of the branching ratio for direct χ_{c2} and χ_{c1}

production in B decays is consistent with the prediction of the color-singlet model [7] and disagrees with the color-evaporation model [9]. In NRQCD framework, our measurement suggests that the color-octet mechanism does not dominate in $B \to \chi_c X$ decays.

We gratefully acknowledge the effort of the CESR staff in providing us with excellent luminosity and running conditions. This work was supported by the National Science Foundation, the U.S. Department of Energy, the Research Corporation, the Natural Sciences and Engineering Research Council of Canada, the A.P. Sloan Foundation, the Swiss National Science Foundation, the Texas Advanced Research Program, and the Alexander von Humboldt Stiftung.

REFERENCES

[1] CDF Collaboration, F. Abe *et al.*, Phys. Rev. Lett. **69**, 3704 (1992); **79**, 572 (1997); **79**, 578 (1997); D0 Collaboration, S. Abachi *et al.*, Phys. Lett. B **370**, 239 (1996).

[2] G. T. Bodwin, E. Braaten and G. P. Lepage, Phys. Rev. D **51**, 1125 (1995).

[3] CDF Collaboration, T. Affolder *et al.*, Report No. FERMILAB-PUB-00-090-E, hep-ex/0004027 (submitted to Phys. Rev. Lett.).

[4] J. F. Amundson, O. J. Eboli, E. M. Gregores, and F. Halzen, Phys. Lett. B **390**, 323 (1997)

[5] M. Beneke, F. Maltoni, and I. Z. Rothstein, Phys. Rev. D **59**, 054003 (1999).

[6] CLEO Collaboration, R. Balest *et al.*, Phys. Rev. D **52**, 2661 (1995).

[7] J. H. Kuhn, S. Nussinov, and R. Ruckl, Z. Phys. **C5**, 117 (1980); J. H. Kuhn and R. Ruckl, Phys. Lett. **135B**, 477 (1984); Phys. Lett. B **258**, 499 (1991).

[8] G. T. Bodwin, E. Braaten, T. C. Yuan, and G. P. Lepage, Phys. Rev. D **46**, 3703 (1992).

[9] G. A. Schuler, Eur. Phys. J. C **8**, 273 (1999).

[10] CLEO Collaboration, Y. Kubota *et al.*, Nucl. Instrum. Meth. Phys. Res. A **320**, 66 (1992).

[11] T.S. Hill, Nucl. Instrum. Meth. Phys. Res. A **418**, 32 (1998).

[12] CERN Program Library Long Writeup W5013 (1993).

[13] Particle Data Group, C. Caso *et al.*, Eur. Phys. J. C **3**, 1 (1998).

[14] BES Collaboration, J. Z. Bai *et al.*, Phys. Rev. D **58**, 092006 (1998).

[15] G.J. Feldman and R.D. Cousins, Phys. Rev. D **57**, 3873 (1998).